Polymer Cholesteric Liquid Crystal Flake Reorientation in an Alternating-Current Electric Field

Introduction

The motion and orientation of nonspherical particles suspended in a host fluid and subjected to an alternating-current (ac) electric field have been well studied theoretically. Because the dielectric properties of the two phases of the suspension differ, charge will start to accumulate at the particle–fluid interface due to Maxwell–Wagner polarization. This charge accumulation induces a dipole moment, which is acted on by the electric field, causing the particle to reorient. Basic electromagnetic theory predicts that a particle in an electric field will orient in the direction corresponding to the lowest energy so as to minimize the potential energy of the system. Typically this requires a dielectric nonspherical particle to align its longest axis parallel to the external field.[1] Because the minimum energy orientation of the particle depends on the shape, the dielectric properties of the host fluid and particle, and the frequency of the ac field, it is possible that a particle will have varying stable orientations at different frequencies. Schwartz *et al*.[2] described the orientation of particles in an ac electric field and considered the conditions for particles with anisotropic dielectric properties or with additional membranes or layers, which is of particular use in the biological sciences. Okagawa *et al*.[3] derived similar equations for a uniform dielectric particle but included the effect of shear flow on the particle motion. Jones did further work in the field of particle electromechanics, including phenomena such as electrophoresis and dielectrophoresis,[4] and a comprehensive review of electromechanical behavior of particles was written by Gimsa.[5] In addition to conducting experiments with biological particles,[6] Miller and Jones investigated highly dielectric particles, such as titanium dioxide.[7] Bostwick and Labes also performed similar experiments using platelets of crystalline nafoxidine hydrochloride.[8] In this article we report on the orientation of highly dielectric polymer cholesteric liquid crystal (PCLC) particles (flakes), suspended in a low-viscosity host fluid. Though much of the theory on particle electromechanics is well supported by experimental work in the biological sciences, relatively little work has been done to study the behavior of highly dielectric particles like PCLC flakes, which have no inherent charge, a low dielectric constant, and a negligible dielectric anisotropy.

PCLC Flakes

PCLC flakes were developed in the 1990s as an alternative to both low-molar-mass cholesteric liquid crystals (LMMLC's) and PCLC thin films. Typical LMMLC molecules can be switched with an electric field, which provides control over their optical properties, but LMMLC's tend to be temperature sensitive and require confining substrates to retain liquid crystalline order. Due to a relatively high glass transition point, PCLC films are not temperature sensitive and can stand alone without substrates. Despite this environmental stability and the usefulness for passive applications, freestanding polymer LC films cannot be manipulated in electric fields. PCLC flakes have the potential to combine two important properties of PCLC films and LMMLC's: environmental stability and electro-optic switching.[9]

PCLC flakes are formed by fracturing thin PCLC films into randomly shaped particles of the order of tens to hundreds of microns.[10] More recently, techniques for processing uniformly shaped flakes with replication methods such as soft lithography have been developed.[11]

An important and unique characteristic of PCLC flakes is that they display selective reflection, a Bragg-like effect resulting from the "helical" molecular structure of PCLC's aligned in the Grandjean texture. Selective reflection causes light of a specific wavelength and (circular) polarization to be reflected from the flake surface. Thus, a large visual effect is created if flakes are viewed off-axis or if they are tipped with respect to normally incident light, whereby the wavelength of selective reflection shifts toward shorter wavelengths and is also diminished. This optical effect provided the motivation for controlling the position, and thus the color and reflectivity, of a PCLC flake using an electric field.[12]

Theory

The response time for flake motion is determined by solving the equation of motion for an ellipsoid, which includes the electrostatic torque exerted on a polarized ellipsoid whose rotation is opposed by a hydrodynamic (viscous) torque from the surrounding host fluid. The mass moment of inertia is neglected because viscosity, and not the flake's inertia, dominates the system. The inertial contribution is several orders of magnitude smaller than contributions from the electrostatic and hydrodynamic torques, i.e., the system is critically damped.

The electrostatic torque $\vec{\Gamma}_E$ is defined as the cross product of the induced dipole moment $\vec{p}$ and the applied electric field $\vec{E}_o$:

$$\vec{\Gamma}_E = \vec{p} \times \vec{E}_o. \tag{1}$$

Here we assume that the particle material has no permanent dipole moment and that the applied electric field is uniform over the flake dimensions. The electric field inside the particle E^+, to which the particle responds, varies with the rotation of the ellipsoid and induces an effective polarization along each ellipsoidal axis i:

$$P_i = \left(\varepsilon_p - \varepsilon_h\right) E_i^+, \tag{2}$$

where

$$E_i^+ = \frac{\varepsilon_h E_{oi}}{\varepsilon_h + A_i\left(\varepsilon_{ii} - \varepsilon_h\right)}, \tag{3}$$

ε_p and ε_h are the dielectric permittivity of the particle and host fluid, respectively, and E_{oi} is the applied electric field component along the particle axis i. Calculations for an electrically isotropic particle can be performed by considering $\varepsilon_{11} = \varepsilon_{22} = \varepsilon_{33} = \varepsilon_p$. The ellipsoid is described by axes lengths a_i, a_j, and a_k, and a depolarization factor A_i must be defined along each axis (where i, j, and k are indices ordered according to the right-handed coordinate system):

$$A_i = \frac{a_i a_j a_k}{2} \int_0^\infty \frac{ds}{\left(s + a_i^2\right)\sqrt{\left(s + a_i^2\right)\left(s + a_j^2\right)\left(s + a_k^2\right)}}. \tag{4}$$

The effective induced dipole moment along each particle axis p_i is

$$p_i = \frac{4\pi}{3} a_i a_j a_k P_i = \frac{4\pi}{3} a_i a_j a_k \varepsilon_h K_i E_{oi}, \tag{5}$$

where we have defined the Clausius–Mosotti factor K_i along each ellipsoidal axis as

$$K_i = \frac{\left(\varepsilon_p - \varepsilon_h\right)}{\left[\varepsilon_h + A_i\left(\varepsilon_p - \varepsilon_h\right)\right]}. \tag{6}$$

Since the dielectric particle and the surrounding medium are not ideal dielectrics, energy dissipation mechanisms such as conduction and dielectric relaxation require that a frequency-dependent complex dielectric constant ε^* be considered:

$$\varepsilon^*(\omega) = \varepsilon - i\frac{\sigma}{\omega}, \tag{7}$$

where ω is the electric field frequency and σ is the electric conductivity. The definitions for K_i^* and p_i^* remain unchanged except that ε_p and ε_h become complex and frequency dependent. Using Eqs. (1) and (5), we find the electrostatic torque Γ_{Ei} along the particle axis i to be

$$\Gamma_{Ei} = \frac{4\pi}{3} a_i a_j a_k \varepsilon_h K_j^* K_k^* \left(A_k - A_j\right) E_{oj} E_{ok}. \tag{8}$$

It is important to note that the ε_h arising from the effective induced dipole moment [Eq. (5)] is not complex because it is not derived from Gauss's law.† The hydrodynamic torque Γ_{Hi} about particle axis i is defined as

$$\Gamma_{Hi} = -\frac{16\pi}{3} a_i a_j a_k \eta_o \frac{\left(a_j^2 + a_k^2\right)}{\left(a_j^2 A_j + a_k^2 A_k\right)} \Omega_i, \tag{9}$$

†See Jones[4] (Appendix G) for a derivation of the induced effective moment of a dielectric ellipsoid, which includes the electrostatic potential external to the ellipsoid.

where η_o is the absolute viscosity of the host fluid and Ω_i is the angular velocity about axis i. The hydrodynamic and electrostatic torques about a specific axis are equated to give the equation of motion for a rotating flake. The angular velocity Ω_i relative to its corresponding axis i is found to be

$$\Omega_i = \frac{\varepsilon_h \varepsilon_o K_j^* K_k^* \left(A_k - A_j\right) E_{oj} E_{ok}}{4\eta_o} \frac{\left(a_j^2 A_j + a_k^2 A_k\right)}{\left(a_j^2 + a_k^2\right)}. \quad (10)$$

We first examine the two-dimensional implication of this result. The two-dimensional coordinate system and reference frame for the flake are defined in Fig.100.51, where θ is the instantaneous angle between the flake's surface normal and the applied electric field.

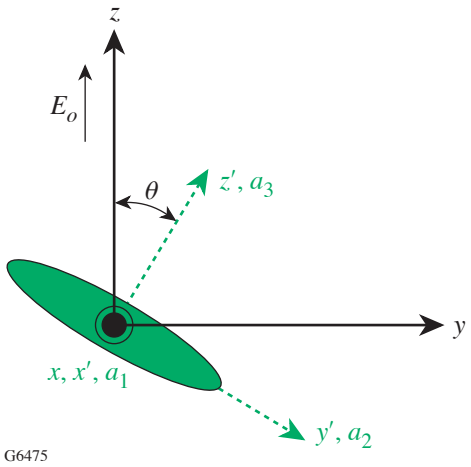

Figure 100.51
The flake reference frame (primed axes) rotates with respect to the laboratory (cell) reference frame (unprimed axes).

If we consider the case where the electric field E_o is applied along the z axis and the flake rotates about axis a_1 (x'), the angular velocity about the flake axis is found to be

$$\frac{d\theta}{dt} = \Omega_1$$

$$= \frac{\varepsilon_h \operatorname{Re}\left\{K_3^* K_2^*\right\}\left(A_3 - A_2\right) E_o^2}{4\eta_o} \frac{\left(a_2^2 A_2 + a_3^2 A_3\right)}{\left(a_2^2 + a_3^2\right)} \sin\theta\cos\theta. \quad (11)$$

We retain the real component of the equation because only the time-averaged term is significant in a heavily damped system where the particle moves slowly compared to the applied electric field. This equation is easily simplified and solved in the form

$$\frac{d\theta}{dt} = \frac{C}{2}\sin 2\theta, \text{ where}$$

$$C = \frac{\varepsilon_h \operatorname{Re}\left\{K_3^* K_2^*\right\}\left(A_3 - A_2\right) E_o^2}{4\eta_o} \frac{\left(a_2^2 A_2 + a_3^2 A_3\right)}{\left(a_2^2 + a_3^2\right)}. \quad (12)$$

Equation (12) can be integrated to obtain an equation for the angle θ at any given time:

$$\tan\theta = \tan\theta_o e^{t/\tau_c}, \quad (13)$$

where θ_o is the initial angle (position) of the flake and $\tau_c = 1/C$ is the time constant for flake relaxation. We can see that for all $\tau_c > 0$, as $t \to \infty$ the angle $\theta \to \pi/2$ is a stable configuration. It is now possible to determine the response time of the flake, or the time needed for θ to approach any final orientation, including $\theta \approx 90°$. The reorientation time from the initial angle θ_o to the current angle θ is given by

$$t = \tau_c \ln\left(\frac{\tan\theta}{\tan\theta_o}\right)$$

$$= \frac{4\eta_o}{\varepsilon_h \operatorname{Re}\left\{K_e^* K_2^*\right\}\left(A_3 - A_2\right) E_o^2} \frac{\left(a_2^2 + a_3^2\right)}{\left(a_2^2 A_2 + a_3^2 A_3\right)} \ln\left(\frac{\tan\theta}{\tan\theta_o}\right). \quad (14)$$

Equation (14) clearly shows that the flake reorientation time should have an inverse quadratic dependence on the applied electric field and a linear dependence on the fluid viscosity. There must be a slight perturbation in the flake position ($\theta_o > 0°$) in order for flake motion to commence.

A three-dimensional model that accounts for the coupling between the components of angular velocity about each axis was developed by Okagawa[3] (see Fig. 100.52). Based on Okagawa's work, the time rate of change of each angle can be found in terms of the components of angular velocity of the

flake defined by Eq. (10), where

$$\frac{d\theta}{dt} = \Omega_1 \cos\psi + \Omega_2 \sin\psi,$$

$$\frac{d\varphi}{dt} = \left(\Omega_2 \cos\psi - \Omega_1 \sin\psi\right)\cos\theta, \tag{15}$$

$$\frac{d\psi}{dt} = \Omega_3 - \left(\Omega_2 \cos\psi - \Omega_1 \sin\psi\right)\cot\theta.$$

Allowing $\psi = 0$ eliminates the angle describing the spin of the flake and simplifies the equations. We solved these equations numerically, and the results validated the two-dimensional analytic solution.

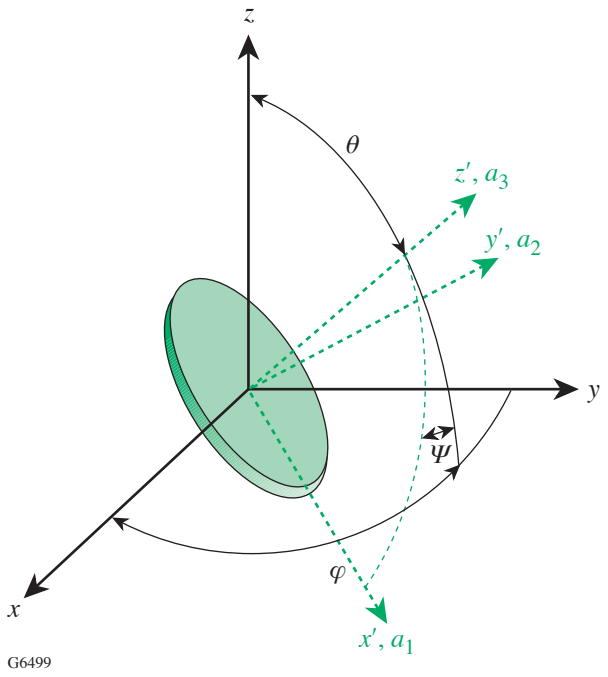

Figure 100.52
Coordinate systems of the (unprimed) laboratory reference frame and the (primed) ellipsoid reference frame. The z' identifies the direction normal to the surface of an oblate particle.

Experimental Procedure

Commercial polycyclosiloxane flakes,[13] typically 6 μm thick, with an arbitrary shape and a selective reflection peak at λ_o = 520 nm (green), were sieved and dried to obtain batches with sizes between 20 and 40 μm [Fig. 100.53(a)]. The PCLC flakes were suspended in two host fluids: a silicone oil (Gelest, DMS-T05) and propylene carbonate (PC) (Aldrich, 99.7% HPLC grade). Though both fluids are transparent, chemically compatible with the PCLC material, and of a comparable density, their dielectric properties varied greatly. The silicone oil had a low dielectric permittivity and was highly insulating ($\varepsilon_h \sim 3\ \varepsilon_o$, $\sigma_h \sim 10^{-11}$ S/m), while the PC had a high dielectric permittivity and was significantly more conductive ($\varepsilon_h \sim 69\ \varepsilon_o$, $\sigma_h \sim 10^{-6}$ S/m). Test cells were constructed using pairs of indium tin oxide (ITO)–coated glass substrates. A mixture of soda lime glass spheres dispersed in a UV-curing epoxy was applied in four corners of one substrate to set the cell gap. Assembled cells were then filled with the flake/host fluid suspension by capillary action and sealed with additional epoxy.

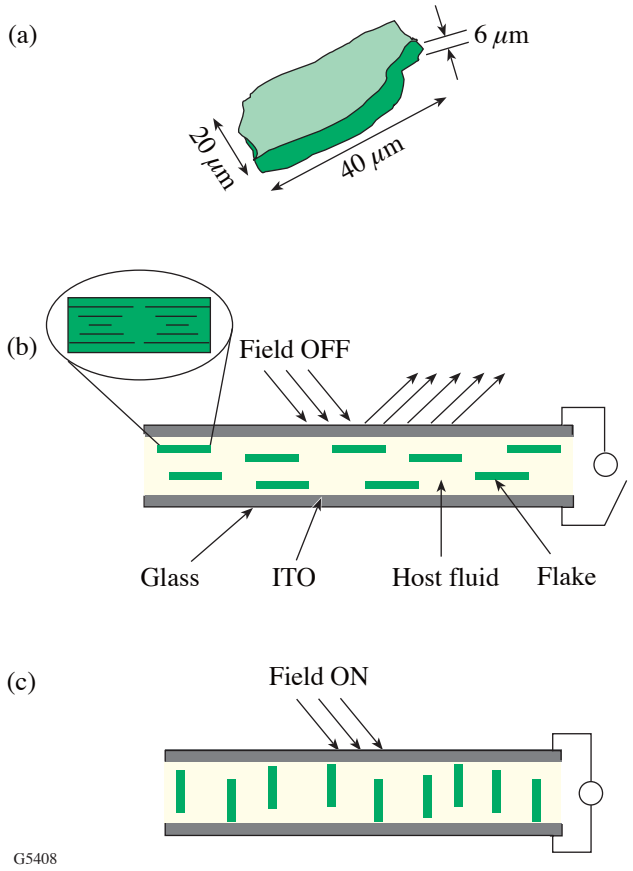

Figure 100.53
Dimensions of a typical irregularly shaped PCLC flake are depicted in (a). Flakes lie approximately parallel to cell substrates when no electric field is applied (b) and appear green due to selective reflection caused by the helical molecular structure of cholesteric liquid crystals, as depicted by the enlarged cross-sectional view of a flake. Flakes reorient with one long axis parallel to the applied field (c). They appear dark since light is no longer reflected off their flat surfaces.

Basic observations were made using a Leitz Orthoplan polarizing microscope. A Panasonic Digital 5100 camera with a timer was used to record flake motion with a time resolution of 100 ms. Data on subsecond flake motion were obtained by detecting the light reflected from the rotating flake surface using a Hamamatsu R905 photomultiplier tube (PMT) coupled to the microscope ocular by means of a fiber optic mounted in a precision fiber coupler. The PMT signal was displayed on one channel of an HP 54520A oscilloscope and directly compared with the field applied to the cell displayed on the second channel. Flake motion was easily detected under near-normal illumination through a 10× objective (N.A. = 0.2). Brightly reflecting flakes lying in the plane defined by the substrates [Fig. 100.53(b)] darkened substantially with only a few degrees of rotation [Fig. 100.53(c)] as they continue reorienting to align parallel with the electric field.

Experimental Results and Discussion

The motion of PCLC flakes in a sinusoidal ac electric field was investigated mainly in the propylene carbonate host system because no motion was observed in the silicone oil host system.* Reorienting PCLC flakes exhibited several characteristics: Flakes consistently rotated about the longest axis, so that the shorter major axis aligned parallel to the applied field direction. Furthermore, flakes with larger aspect ratios (length to width) reoriented more quickly than flakes of a comparable size, but with a smaller aspect ratio. Once the driving field was turned off, flakes returned to their initial position in the plane of the cell. This approximate 90° relaxation required anywhere from several seconds to several minutes to be completed. There was also a gradual and approximately linear increase in response time over the lifetime of the PCLC flake test device during test periods of 2 days.

Both the electric-field frequency and magnitude affected flake reorientation times. Flake motion was seen within a specific frequency bandwidth (~10 Hz to 1 kHz), above and below which flake reorientation did not occur (Fig. 100.54). Motion for a typical flake was detected in fields as low as 5 $mV_{rms}/\mu m$, but fields above 30 $mV_{rms}/\mu m$ were required for flake reorientation to occur on a subsecond time scale. The inverse quadratic dependence on the electric field was observed clearly as the flake reorientation time was tested as a function of applied voltage (Fig. 100.55).

From Eq. (14), it is clear that the measured inverse quadratic dependence of the response time on the applied field supports the theoretical model predictions of the previous section. The dependence on the flake shape is more complicated, but a study of seven specific PCLC flakes suspended in PC and observed in a 10.4-$mV_{rms}/\mu m$ field at 50 Hz showed clearly that the reorientation time decreases as the aspect ratio increases. This shape-dependent behavior was also as predicted by the theoretical model (Fig. 100.56).

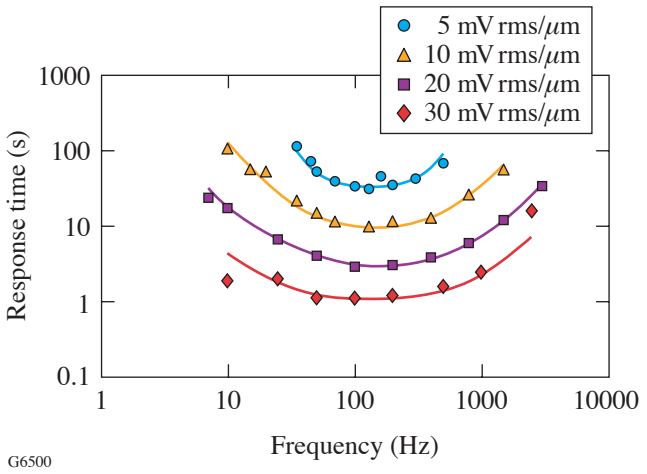

Figure 100.54
The characteristic time response of a representative PCLC flake as a function of frequency at specific electric-field values. Lines are drawn to guide the eye. Similar behavior was observed for dozens of individual flakes.

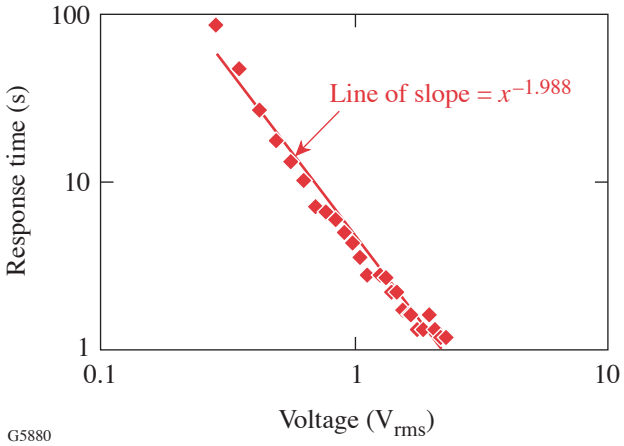

Figure 100.55
The average response time of several flakes exhibited an inverse quadratic dependence on the applied voltage. The standard deviation of 10% is of the order of the size of the data points. Data was collected at 50 Hz.

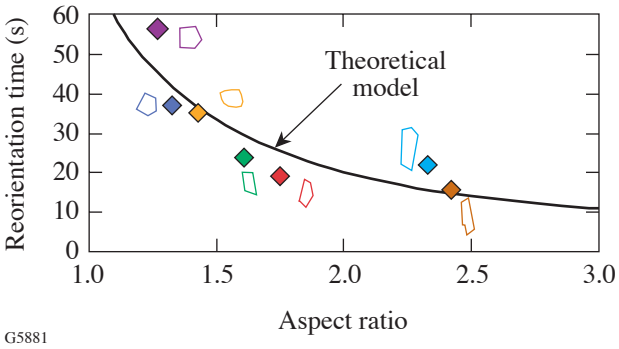

Figure 100.56
A correlation between response time and flake size and shape was observed. Flakes with the largest aspect (length to width) ratio reorient the fastest.

Though many of the observations above were supported by theory, two results were not supported by previous theoretical work. For flakes with axes $a_1 > a_2 > a_3$, we expected that the flakes would align with their longest axis a_1, parallel to the electric field. Instead, we observed that the flakes consistently aligned with the shorter major axis a_2, parallel to the applied electric field. Schwarz[2] used the Clausius–Mosotti factor K_i, which measures the energy of the ellipsoid when it is oriented with its i axis parallel to the field, to predict the stable orientation of the particle. He suggested that the axis with the smallest K_i would align parallel to the applied field. Using the following typical parameters we found that, for all frequencies, K_1 had the smallest value: $\varepsilon_h \sim 69\ \varepsilon_o$; $\sigma_h \sim 10^{-6}$ S/m; $\varepsilon_p \sim 2.89\ \varepsilon_o$; $\sigma_p < 10^{-11}$ S/m; $a_1 = 35\ \mu$m; $a_2 = 15\ \mu$m; and $a_3 = 5\ \mu$m. This result indicated that the longest axis a_1 should align with the electric field, which is contrary to our observations.

Jones produced a chart for determining the preferred axis alignment based on a combination of signs of the torque terms for each axis. In practice, only the sign of the real component of the Clausius–Mosotti term $\left(K_j^* K_k^*\right)$ was considered because it is proportional to the torque [Eq. (8)]. Considering only the Clausius–Mosotti terms excludes the difference in depolarization factors (A_k–A_j). This difference term can flip the sign of the torque if A_k is less than A_j. We used the Jones chart, initially considering just $\mathrm{Re}\left\{K_j^* K_k^*\right\}$ and then including $\left(A_k - A_j\right)\mathrm{Re}\left\{K_j^* K_k^*\right\}$, to predict which flake axis would align with the electric field. Neither method produced results that correspond with our observations.

To predict which particle axis would align parallel to the electric field, we found it necessary to consider not only the electric torque but also contributions of the viscous drag (hydrodynamic torque), which become more important as the lengths of the two major axes become more similar. One way to include the effects of the viscous drag was to compare the magnitude of the angular velocity components about each axis. Assuming that the particle reorients about the axis with the largest angular velocity component, and for the material parameters given above, we found that a flake lying nearly parallel to the substrate will reorient about the longest axis a_1, so that the shorter of the two major axes, a_2, aligns parallel to the electric field, just as we had observed. This result will be true unless the flake's initial condition is already tilted largely about the shorter axis a_2.

The second result not supported by theoretical work arose when we compared our model of flake reorientation times with electric-field frequency. Initially we used the real part of the Clausius–Mosotti factor in the electric torque term, and the resultant theoretical model showed a weak frequency dependence. The characteristic S shape of the theoretical curve (Fig. 100.57, insert) shifted toward higher (lower) frequencies when host fluids with a higher (lower) conductivity were modeled. However, the model predictions using the S-shaped curve agreed poorly with the experimental data. The data showed a minimum reorientation time at a specific frequency above and below which the reorientation times increased. The model based on the real component of the Clausius–Mosotti factor corresponded well only with the general order of magnitude of the flake reorientation time (Fig. 100.57).

Because the frequency dependence of the reorientation time data resembled the typical dispersion spectrum for the imaginary part of the dielectric constant, we also explored using the imaginary part of the Clausius–Mosotti factor in our model. Use of the imaginary component produced a theoretical curve with a U shape that agreed well with the shape of the experimental data. However, the predicted response times were more than an order of magnitude higher than those observed.

The imaginary component of the Clausius–Mosotti term is typically used only in equations describing electro-rotation, which is the continuous rotation of a particle in the presence of a rotating electric field.[4] When there is a rotating electric field, it is necessary to consider the phase angle of K_i^*, which represents a (constant) phase lag between the applied electric field and the induced moment. Physically, the induced dipole lags behind the applied field by an angle related to the time necessary for the dipole moment to form as charge builds up at the particle–fluid interface. The angular velocity of the particle will vary from the angular velocity of the rotating electric field, and the particle will typically be rotating more slowly (due to

the viscous drag) than the surface charge on the particle that produced the induced dipole.

Since the conditions for PCLC flake reorientation include a linear electric field with which the induced dipole moment eventually aligns, we cannot assume a constant phase between these two vectors. However, the imaginary component also helps quantify the time required to induce the dipole moment, which might explain why using this term models the frequency-dependent behavior of the flake reorientation time so well.

The discrepancy between the predicted and observed reorientation times implies that either the viscosity of the host fluid is much lower or the *effective* electric field (to which the flake responds) is significantly larger than the applied electric field. The viscosity of propylene carbonate is well known, so it is possible that the effective electric field is larger. This possibility would imply that perhaps another electric-field–dependent term has not been considered in the expression for the electric torque.

Summary

We have observed that flakes suspended in a moderately conductive host fluid, such as propylene carbonate, reorient about their longest axis to align the shorter major axis parallel to the applied electric field. This observation was contrary to most theories on particle reorientation, which predict that the longest axis will align with the applied electric field. We compared the components of the angular velocity about each axis, which include important parameters such as particle shape and host fluid viscosity, hypothesizing that the flake will rotate about the axis with the largest angular-momentum component. This approach was found to support our observations. Other standard characteristics of PCLC flake motion, such as the inverse quadratic dependence on the electric field and the tendency for longer, asymmetric flakes to reorient faster, were theoretically predicted and agreed with our experimental observations.

The frequency dependence of the flake reorientation time was difficult to model because it is unclear whether the real or the imaginary component of the Clausius–Mosotti term should

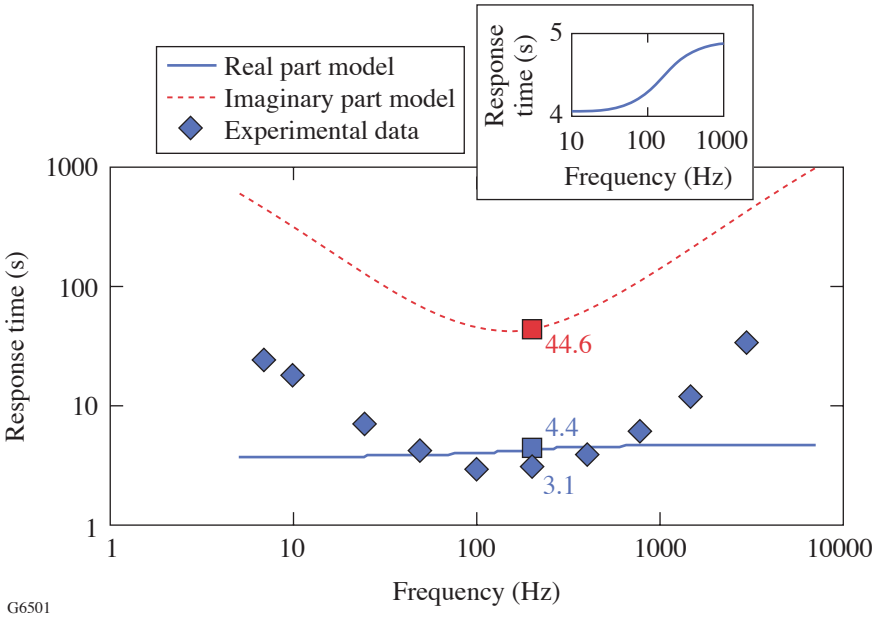

Figure 100.57
A comparison of experimental data and a theoretical model based on experimental parameters (E_o = 20 mV/μm; η_o = 2.9 cP; $\varepsilon_h \sim 69\ \varepsilon_o$; $\varepsilon_p \sim 2.89\ \varepsilon_o$; $\sigma_p < 10^{-12}$ S/cm) and estimated values ($\sigma_h \sim 10^{-6}$ S/m; a_1 = 35 μm; a_2 = 15 μm; a_3 = 5 μm). The open squares designate the theoretical values for comparison with the experimental data at 200 Hz. The insert shows the frequency dependence of the model that utilized the real component of the Clasius–Mosotti term on an expanded semi-log scale.

be used. Using the real component, which is a widely accepted approach, the model predicts reorientation times on the same order of magnitude as the observed reorientation times; however, the frequency dependence does not match the experimental data. This discrepancy is partially resolved by using the imaginary component in the model. The theoretical curve based on the imaginary component shows a minimum reorientation time at a specific electric-field frequency, which corresponds well with experimental data. This alternate method also predicts, however, reorientation times approximately an order of magnitude higher than what we observed. Future research will require investigating effects of electro-osmosis, double layers, and rotating electric fields. Similar frequency-dependent particle behavior has been observed when a rotating electric field causes a particle to rotate. The particle rotation results from a phase difference between the electric-field–induced polarization and the rotating field, thereby requiring theory to consider the imaginary component of the Clausius–Mosotti term.[14]

The ability to reorient, or switch, PCLC flakes provides a way to control their unique optical and polarizing properties with an electric field. Electro-optic devices based on switching PCLC flakes are useful in a broad class of applications in information displays, optics, and photonics. A PCLC flake device is of particular interest in the display industry (large-area signs, automobile dashboards, heads-up displays, and "electronic paper") because it easily provides both color and polarization without the use of filters and polarizers, which reduce brightness and add to the production cost. Possible applications in optics and photonics include switchable and tunable optical retardation or modulation elements for polarized light at any desired wavelength or bandwidth. It is also possible to produce conformal PCLC flake coatings for use in either decorative applications or military applications such as camouflage, document security, anti-counterfeiting, and object tagging and identification. Thus reorienting PCLC flakes has an unlimited number of potential applications, many of which have yet to be conceived.

ACKNOWLEDGMENT

The authors would like to acknowledge the Laboratory for Laser Energetics at the University of Rochester for continuing support. This work was also supported by the U.S. Department of Energy Office of Inertial Confinement Fusion under Cooperative Agreement No. DE-FC52-92SF19460, the University of Rochester, and the New York State Energy Research and Development Authority. The support of DOE does not constitute an endorsement by DOE of the views expressed in this article.

REFERENCES

*Flake motion in the silicone oil was observed only when dc fields were applied, whereby typical flake motion was random and uncontrolled. The system relaxation time was very long due to the low conductivity of the silicone oil host, which prevented a stable dipole moment from being induced.

1. J. A. Stratton, *Electromagnetic Theory*, 1st ed., International Series in Physics (McGraw-Hill, New York, 1941).

2. G. Schwarz, M. Saito, and H. P. Schwan, J. Chem. Phys. **43**, 3562 (1965).

3. A. Okagawa, R. G. Cox, and S. G. Mason, J. Colloid Interface Sci. **47**, 536 (1974).

4. T. B. Jones, *Electromechanics of Particles* (Cambridge University Press, New York, 1995).

5. J. Gimsa, Bioelectrochemistry **54**, 23 (2001).

6. R. D. Miller and T. B. Jones, Biophys. J. **64**, 1588 (1993).

7. R. D. Miller, "Frequency-Dependent Orientation of Lossy Dielectric Ellipsoids in AC Electric Fields," Ph.D. thesis, University of Rochester, 1989.

8. B. D. Bostwick and M. M. Labes, Appl. Phys. Lett. **45**, 358 (1984).

9. K. L. Marshall, T. Z. Kosc, S. D. Jacobs, S. M. Faris, and L. Li, U.S. Patent No. 6,665,042 B1 (16 December 2003).

10. E. M. Korenic, S. D. Jacobs, S. M. Faris, and L. Li, Mol. Cryst. Liq. Cryst. **317**, 197 (1998); S. M. Faris, U.S. Patent No. 5,364,557 (15 November 1994).

11. A. Trajkovska-Petkoska, R. Varshneya, T. Z. Kosc, K. L. Marshall, and S. D. Jacobs, "Enhanced Electro-Optic Behavior for Shaped Polymer Cholesteric Liquid Crystal (PCLC) Flakes Made by Soft Lithography," to be published in Advanced Functional Materials.

12. T. Z. Kosc, K. L. Marshall, S. D. Jacobs, J. C. Lambropoulos, and S. M. Faris, Appl. Opt. **41**, 5362 (2002).

13. Wacker-Chemie, Consortium für Electrochemische Industrie GmbH, Zielstattstrasse 20, D-81379, München, Germany.

14. W. M. Arnold and U. Zimmermann, J. Electrost. **21**, 151 (1988).